



ELSEVIER

Contents lists available at ScienceDirect

Comptes Rendus Physique

www.sciencedirect.com



URSI-France 2018 Workshop: Geolocation and navigation / Journées URSI-France 2018 : Géolocalisation et navigation

Bayesian fusion of GNSS, ITS-G5 and IR-UWB data for robust cooperative vehicular localization

*Fusion bayésienne de données GNSS, ITS-G5 et IR-UWB pour des applications robustes de localisation véhiculaire coopérative*Gia Minh Hoang^a, Benoît Denis^{b,*}, Jérôme Härrri^c, Dirk Slock^c^a Orolia Spectracom, Parc Technopolis, 3, avenue du Canada, 91974 Les Ulis cedex, France^b CEA-Leti, Minatoc Campus, 17, rue des Martyrs, 38054 Grenoble cedex 9, France^c EURECOM, SophiaTech Campus, 450, route des Chappes, 06904 Sophia Antipolis, France

ARTICLE INFO

Article history:

Available online xxxx

Keywords:

Bayesian data fusion

Cooperative localization

Impulse Radio-Ultra WideBand (IR-UWB)

ITS-G5

Vehicle-to-Vehicle (V2V) data communications

Vehicular Ad hoc NETWORK (VANET)

Mots-clés :

Fusion de données hybrides

Localisation coopérative

Radio impulsionnelle ultra-large bande (IR-UWB)

ITS-G5

Communications inter-véhicules (V2V)

Réseau véhiculaire ad hoc (VANET)

ABSTRACT

In the automotive domain, Cooperative Localization (CLoc) is a new promising paradigm that aims at outperforming conventional Global Navigation Satellite Systems (GNSS) in terms of positioning accuracy, robustness, and service continuity, by relying on Vehicle-to-Vehicle (V2V) communications and hybrid data fusion. However, the growing number and the variety of the sensors aboard vehicles raise unprecedented challenges, especially in the context of distributed fusion approaches. This paper thus compares parametric and nonparametric Bayesian data fusion engines (e.g., based on cooperative variants of the Extended Kalman Filter (EKF) and Particle Filter (PF), respectively), while validating a CLoc scheme suitable to Vehicular Ad Hoc Networks (VANETs). More particularly, *absolute* position information from both onboard GNSS receiver and ITS-G5 V2V messages, as well as *relative* distance measurements based on the Impulse Radio-Ultra-Wideband (IR-UWB) technology, are combined into a single location solution that is hopefully more robust and more accurate than that of standalone GNSS. First, we investigate V2V ranging accuracy on a highway under real mobility conditions. In the same environment, we then provide offline validations of CLoc positioning, confirming significant performance gains through cooperation over conventional GNSS, even in case of poor initialization. In this specific context, the PF solution is thus shown to yield even better accuracy in comparison with EKF, thanks to its fine robustness against faced non-linear dynamics and non-Gaussian noise processes. Finally, we illustrate the resilience of the proposed solution under temporary GNSS denial.

© 2019 Académie des sciences. Published by Elsevier Masson SAS. This is an open access article under the CC BY-NC-ND license (<http://creativecommons.org/licenses/by-nc-nd/4.0/>).

R É S U M É

Dans le domaine automobile, la localisation coopérative (CLoc) apparaît aujourd'hui comme un paradigme particulièrement prometteur, qui doit permettre d'améliorer les performances des systèmes conventionnels de navigation par satellite (GNSS) en termes de précision de positionnement et de continuité de service, en mettant à profit les

* Corresponding author.

E-mail addresses: gia-minh.hoang@orolia.com (G.M. Hoang), benoit.denis@cea.fr (B. Denis), haerri@eurecom.fr (J. Härrri), slock@eurecom.fr (D. Slock).<https://doi.org/10.1016/j.crhy.2019.03.004>1631-0705/© 2019 Académie des sciences. Published by Elsevier Masson SAS. This is an open access article under the CC BY-NC-ND license (<http://creativecommons.org/licenses/by-nc-nd/4.0/>).

communications sans fil entre véhicules (V2V) ainsi que des techniques avancées de fusion de données. Toutefois, le nombre grandissant et la variété des capteurs disponibles à bord des véhicules donnent lieu à des questions de recherche sans précédent, a fortiori dans un contexte de traitements distribués. Dans cet article, on se propose de comparer des techniques paramétriques et non paramétriques de fusion bayésienne (typiquement, des variantes coopératives du filtre de Kalman étendu (EKF) et du filtre particulaire (PF)), permettant de résoudre ce problème de localisation coopérative dans un contexte de réseaux véhiculaires ad hoc (VANET). Plus spécifiquement, on cherche à fusionner une information locale de position absolue, telle que celle délivrée par le récepteur GNSS embarqué, avec les positions présumées de véhicules voisins (comprises dans des messages V2V reposant sur le standard de communication ITS-G5), d'une part, et avec des mesures de distances relatives vis-à-vis de ces mêmes voisins (en s'appuyant sur la technologie radio impulsionnelle ultra-large bande (IR-UWB)), d'autre part. Par le biais de cette fusion coopérative, on s'attend à atteindre des niveaux de précision et de robustesse de localisation supérieurs à ceux d'un système GNSS indépendant. Dans un premier temps, on évalue ici la qualité des mesures de distances point à point entre véhicules, pour des conditions de mobilité réelles sur autoroute. Dans ce même environnement, on fournit ensuite une validation expérimentale complète (à temps différé) du concept de positionnement CLoc, confirmant l'intérêt de la coopération entre véhicules, y compris en cas d'initialisation grossière de la position du véhicule. À cette occasion, on met également en évidence l'apport du filtre particulaire, qui semble être mieux adapté (que le filtre EKF) aux dynamiques non linéaires et non gaussiennes rencontrées. Pour finir, on illustre la résilience de la solution proposée vis-à-vis de pertes temporaires du signal GNSS.

© 2019 Académie des sciences. Published by Elsevier Masson SAS. This is an open access article under the CC BY-NC-ND license

(<http://creativecommons.org/licenses/by-nc-nd/4.0/>).

1. Introduction

Accurate and reliable location awareness in fleets of road vehicles will play a vital role for future Cooperative Intelligent Transport System (C-ITS) applications and services, such as traffic management, autonomous driving and maneuvers negotiation, advanced safety mechanisms for road users or the vehicular Internet of Things (IoT) through geo-referenced crowd sensing. Although the Global Navigation Satellite System (GNSS) is still today the most common and accessible choice in this vehicular context, it fails in fulfilling most C-ITS application requirements in terms of accuracy (say, sub-metric), robustness, and availability. However, in a reasonably short term, all vehicles should enjoy global wireless connectivity through Vehicle-to-Infrastructure (V2I) and/or Vehicle-to-Vehicle (V2V) communication links (e.g., forming Vehicular Ad hoc NETWORKS (VANETs) in the latter case). Accordingly, they could exchange intentional information, maximize their field of view, improve their mutual awareness of the driving environment and assist each other. By leveraging on the supplementary information available with such Vehicle-to-Everything (V2X) connectivity (and notably, from V2V data), Cooperative Localization (CLoc) is thus expected to outperform conventional standalone (i.e. single-vehicle) localization techniques [1,2]. The general principle of vehicular CLoc can be summarized in two main phases.

In the first phase, each vehicle piggybacks position-dependent data (e.g., at least its *absolute* GNSS position) in a “Beacon” broadcast over V2X communication links.¹ In the second phase, through the reception of these “Beacons”, a given “Ego” vehicle becomes aware of the *absolute* position estimates of its neighbors. One optional task consists in using the signal statistics of these received “Beacons” to opportunistically infer *relative* range- and/or position-dependent information. Another alternative is to use a side radio technology devoted to accurate ranging. Finally, so as to refine initial GNSS readings, data fusion algorithms are in charge of combining these multiple sources of information, as shown in Fig. 1:

- data from other entities representing their local observations through V2X communications (e.g., GNSS data, sensor data, etc.);
- data from communication signals (e.g., Received Signal Strength Indicator (RSSI), Time of Arrival (ToA), Time of Flight (ToF), Time Difference of Arrival (TDoA), Phase Difference of Arrival (PDoA), Angle of Arrival (AOA), etc.);
- data from onboard sensors (e.g., GNSS data, sensor data, digital map, etc.).

Extensive research efforts have been committed to make use of explicit V2V location-dependent radio measurements based on mature and low-cost standards, as well as further information issued by on-board kinematic sensors (e.g., speed, acceleration, heading, etc.). In [3], a simplified CLoc fusion architecture based on an Extended Kalman Filter (EKF) combines GNSS data with V2V range measurements in a star topology (thus, avoiding the exchange of vectors of range measure-

¹ A so-called “Beacon” herein depicts a message periodically broadcast by each node, while V2X refers to any technology capable of Device-to-Device communication in a vehicular context.

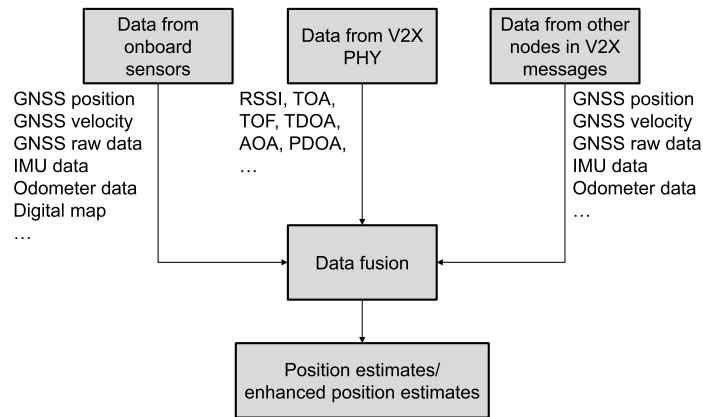


Fig. 1. Simplified CLoc dataflow at an “Ego” vehicle, where PHY stands for the PHYsical layer of the radio used to infer range-/location-dependent measurements (i.e. out of legacy V2V data communications (e.g., ITS-G5) or relying on a side ranging-devoted radio technology (e.g., IR-UWB)).

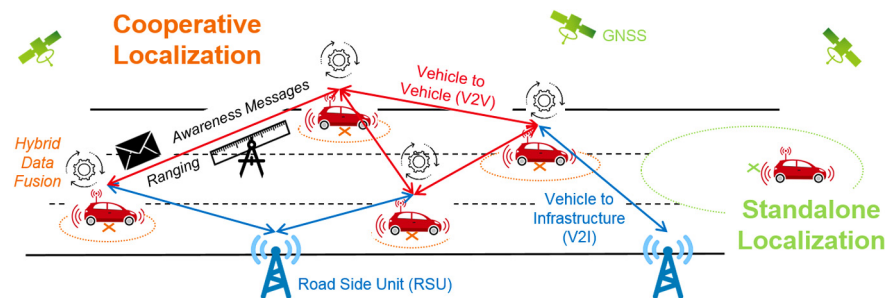


Fig. 2. CLoc principle illustration: the “Ego” vehicle performs data fusion after receiving ITS-G5 V2X CAM messages and performing IR-UWB V2V ranging measurements with respect to single-hop “Virtual Anchors”, thus improving positioning accuracy (in comparison with standalone GNSS localization).

ments). Another integrated fusion architecture based on a modified cubature KF in [4] fuses GNSS data with both V2V ITS-G5 Doppler shifts and RSSI-based ranges. In [5], the GNSS data is also fused with the RSSI of V2V messages such as ITS-G5 Cooperative Awareness Messages (CAMs), along with inertial sensor data from driver’s smartphone and a priori map information. A two-step Bayesian framework has been proposed, including an Unscented Kalman Filter (UKF) in charge of pre-processing the inertial-based heading, whereas a core Particle Filter (PF) is used to fuse all the remaining sources of information. Real-world experiments have even been conducted in the city of Porto. In another similar solution referred to as Virtual Anchors assisted CLoc (VA-CLoc) [6–9], each vehicle considers its neighbors as potential “Virtual Anchors” (i.e. mobile anchors with approximate knowledge of their own positions). Again, all vehicles first encapsulate their latest absolute positions (typically their last fusion results) in V2V ITS-G5 CAM messages. Various cooperative formulations of both EKF and PF have thus been considered at the “Ego”² vehicle to fuse on-board GNSS data with V2V range-dependent radio information (see Fig. 2). Finally, each vehicle contributes to improve the localization of its neighbors by broadcasting in return its own fusion results within subsequent beacons. In terms of incorporated V2V radio measurements, the RSSI associated with received CAMs has also been considered as a starting point in [6,7], for simplicity. Preliminary experimental validations in a highway scenario [10] have already shown significant gains in comparison with standard GNSS performance (e.g., reducing the 2-D location error by 50% in average), even though an in-site prior calibration of the path loss model parameters is required. All in all, none of the solutions accounted above could really meet the sub-metric accuracy requirement.

More recently, accurate V2V range measurements based on Impulse Radio - Ultra Wideband (IR-UWB) Round Trip - Time of Flight (RT-ToF) estimation have been incorporated in the problem, instead of using ITS-G5 RSSI metrics, while keeping ITS-G5 uniquely for V2V communications. The IR-UWB technology, which inherently benefits from fine time resolution due to a large instantaneous bandwidth, can indeed theoretically provide sub-metric peer-to-peer ranging accuracy (typically, from a few cm to a few tens of cm) through precise ToA estimation and multi-way protocol transactions. But in addition to the ranging capability, the impulse nature (with typical pulse durations of approximately 1 ns) and the very low power spectral density of the transmitted signals (i.e. at most -41.3 dBm/MHz, expressed in terms of effective isotropically radiated power) on the one hand, as well as the application of spread-spectrum techniques (typically, coding the temporal position and/or the amplitude of sequences of transmitted pulses) on the other hand, make IR-UWB particularly immune to

² The so-called “Ego” vehicle herein performs fusion at a given point in time. Given the decentralized nature of VA-CLoc, the roles of “Ego” and “Virtual Anchors” are interchangeable among cooperating vehicles over time.

narrow-band unintentional interference, intentional jamming and/or interceptions. This is typically the case within coherent transceivers operating at central frequencies between 3 and 5 GHz and occupying bandwidths between 500 MHz and 1 GHz, such as that used in our experiments [11]. Using IR-UWB in CLoc, even more promising gains have thus been shown by means of simulations in pathological cases such as narrow streets or GNSS-altered environments [8,9]. However, to the best of our knowledge, only rare field trials have been conducted so far with V2V IR-UWB range measurements in real driving conditions. In [12], aiming at improving mostly the horizontal positioning accuracy in a group of three vehicles, Differential GNSS (DGNSS) pseudoranges have been fused with V2V IR-UWB range measurements and bearing measurements using an EKF in different scenarios. However, these preliminary tests have shown that the combination of DGNSS with IR-UWB could be occasionally counterproductive, or even worse than standalone DGNSS. Timing errors corrupting the IR-UWB data or erratic ranging behaviors under high-speed mobility (e.g., caused by synchronization issues) could be incriminated as plausible reasons. The discrepancy between large prior positioning errors and very accurate ranging observations could also lead to violate the usual operating conditions of EKF (or PF) in some specific cases, as illustrated in [9]. Besides, the fusion between IR-UWB and standard mass-market GNSS has not been really investigated yet (but mostly with DGNSS).

In this paper, we first generalize the previous VA-CLoc problem into a generic Bayesian fusion framework supporting cooperative variants of both PF and EKF. We also account for new offline proof-of-concept validations, relying on a demonstration platform integrating ITS-G5, GNSS and IR-UWB technologies. We first evaluate the 1-D precision of IR-UWB V2V range measurements under typical vehicular mobility. We then illustrate the nominal performance gains achieved in terms of positioning beyond standard GNSS in the steady-state fusion regime (i.e. with reliable initialization and reliable information from neighboring vehicles), as well as under erroneous initialization and GNSS denial at the “Ego” vehicle. On this occasion, we show the superiority of PF to overcome the highly erratic (non-Gaussian) observation noise affecting IR-UWB range measurements, as well as observations non-linearity.

The remainder of the paper is organized as follows. In Section 2, we recall the CLoc problem formulation, as well as the proposed fusion solutions based on EKF and PF. In Section 3, we describe the experimental setting and the tested scenario. Then in Section 4, we present the corresponding offline validation results. Finally, Section 5 concludes the paper.

2. Problem formulation and proposed fusion framework

2.1. Overall system model

The state vector of vehicle i includes its 2-D coordinates $\mathbf{x}_{i,k} = (x_{i,k}, y_{i,k})^\dagger$ and velocities $\mathbf{v}_{i,k} = (v_{i,k}^x, v_{i,k}^y)^\dagger$, all expressed at discrete time step k according to a local timeline.³

2.1.1. Mobility model

We first consider a generic discrete-time 2-D mobility model, as follows:

$$\mathbf{x}_{i,k+1} = \mathbf{A}\mathbf{x}_{i,k} + \mathbf{B}(\Delta T)\mathbf{v}_{i,k} + \mathbf{C}(\Delta T)\mathbf{w}_{i,k} \quad (1)$$

where $\mathbf{A} = \mathbf{I}_2$, $\mathbf{B}(\Delta T) = \Delta T\mathbf{I}_2$, $\mathbf{C}(\Delta T) = \frac{\Delta T^2}{2}\mathbf{I}_2$, \mathbf{I}_2 the identity matrix of size 2×2 , ΔT the time step, $\mathbf{w}_{i,k} = (w_{i,k}^x, w_{i,k}^y)^\dagger \sim \mathcal{N}((0, 0)^\dagger, \mathbf{Q}_{i,k})$ the 2-D process noise vector and $\mathbf{Q}_{i,k}$ the related covariance. This model is used to predict and resynchronize “Ego’s” and neighbors’ locations.

2.1.2. Observation model

GNSS absolute position. The 2-D estimated GNSS position, $\mathbf{x}_{i,k}^{\text{GNSS}} = (z_{i,k}^x, z_{i,k}^y)^\dagger$, is assumed to be affected by an additive noise term $\mathbf{n}_{i,k}^{\text{GNSS}} = (n_{i,k}^x, n_{i,k}^y)^\dagger$, which is independent and identically distributed (i.i.d.) centered Gaussian [13] with standard deviation σ_{GNSS} , as follows:

$$z_{i,k}^x = x_{i,k} + n_{i,k}^x, \quad z_{i,k}^y = y_{i,k} + n_{i,k}^y \quad (2)$$

IR-UWB V2V ranges. Through a cooperative ranging protocol (e.g., based on ToA estimation and multi-way handshake transactions), node i can estimate the V2V distance $z_{j \rightarrow i,k}$ with respect to node j :

$$z_{j \rightarrow i,k} = \|\mathbf{x}_{i,k} - \mathbf{x}_{j,k}\| + n_{j \rightarrow i,k} \quad (3)$$

where $n_{j \rightarrow i,k}$ is an i.i.d. centered Gaussian noise term with standard deviation σ_{UWB} .

We depict the stacked states of “Virtual Anchors” as $\mathbf{x}_{\mathcal{S} \rightarrow i,k} = \{\mathbf{x}_{j,k} | \forall j \in \mathcal{S} \rightarrow i,k\}$, the augmented state as $\mathbf{x}_{i \cup \mathcal{S},k} = (\mathbf{x}_{i,k}^\dagger, \mathbf{x}_{\mathcal{S} \rightarrow i,k}^\dagger)^\dagger$, the vector of V2V ranges as $\mathbf{z}_{\mathcal{S} \rightarrow i,k} = \{z_{j \rightarrow i,k} | \forall j \in \mathcal{S} \rightarrow i,k\}$, and the full observation vector as:

³ Due to asynchronously sampled time instants, the index k is different from one vehicle to others. The subscript of the “Ego” is herein dropped for brevity.

Algorithm 1 EKF-based fusion (iteration k , “ego” vehicle i).

- 1: **CAM Collection:** Receive CAMs from the set $\mathcal{S}_{\rightarrow i,k}$ of perceived neighbors, extract the Gaussian beliefs $\{\hat{\mathbf{x}}_{j,k}, \mathbf{P}_{j,k}\}$, the velocity $\mathbf{v}_{j,k}$, the timestamps $t_{j,k}$ and (optionally) mobility parameters like $\mathbf{Q}_{j,k}$, $j \in \mathcal{S}_{\rightarrow i,k}$.
- 2: **Prediction and data synchronization:** Perform prediction of both “ego” and neighboring beliefs based on mobility prediction models at the “ego” estimation instant $t_{i,k}$

$$\begin{aligned} \hat{\mathbf{x}}_{i,k|k-1} &= \mathbf{A}\hat{\mathbf{x}}_{i,k-1} + \mathbf{B}(\Delta T)\mathbf{v}_{i,k-1}, \\ \mathbf{P}_{i,k|k-1} &= \mathbf{A}\mathbf{P}_{i,k-1}\mathbf{A}^\dagger + \mathbf{C}(\Delta T)\mathbf{Q}_{i,k}\mathbf{C}(\Delta T)^\dagger, \\ \hat{\mathbf{x}}_{j,k_i|k} &= \mathbf{A}\hat{\mathbf{x}}_{j,k} + \mathbf{B}(\Delta T_k^{i,j})\mathbf{v}_{j,k}, \\ \mathbf{P}_{j,k_i|k} &= \mathbf{A}\mathbf{P}_{j,k}\mathbf{A}^\dagger + \mathbf{C}(\Delta T_k^{i,j})\mathbf{Q}_{j,k}\mathbf{C}(\Delta T_k^{i,j})^\dagger, \\ \Delta T_k^{i,j} &= t_{i,k} - t_{j,k}, \quad j \in \mathcal{N}_{\rightarrow i,k}. \end{aligned}$$

- 3: **Correction:** Aggregate the predicted states $\hat{\mathbf{x}}_{j,k_i|k}$ and covariance matrices $\mathbf{P}_{j,k_i|k}$, $j \in \mathcal{S}_{\rightarrow i,k}$ (by constructing block diagonal matrix) to obtain $\hat{\mathbf{x}}_{\mathcal{S}_{\rightarrow i,k}|k^-}$ and $\mathbf{P}_{\mathcal{S}_{\rightarrow i,k}|k^-}$ respectively then

$$\begin{aligned} \hat{\mathbf{x}}_{i \cup \mathcal{S},k|k^-} &= (\hat{\mathbf{x}}_{i,k|k-1}^\dagger, \hat{\mathbf{x}}_{\mathcal{S}_{\rightarrow i,k}|k^-}^\dagger)^\dagger, \\ \mathbf{P}_{i \cup \mathcal{S},k|k^-} &= \begin{pmatrix} \mathbf{P}_{i,k|k-1} & \mathbf{0} \\ \mathbf{0} & \mathbf{P}_{\mathcal{S}_{\rightarrow i,k}|k^-} \end{pmatrix}, \\ \mathbf{H}_{i,k} &= \left. \frac{\partial \mathbf{h}_{i,k}}{\partial \mathbf{x}_{i \cup \mathcal{S},k}} \right|_{\mathbf{x}_{i \cup \mathcal{S},k} = \hat{\mathbf{x}}_{i \cup \mathcal{S},k|k^-}}, \\ \mathbf{K}_{i,k} &= \mathbf{P}_{i \cup \mathcal{S},k|k^-} \mathbf{H}_{i,k}^\dagger (\mathbf{H}_{i,k} \mathbf{P}_{i \cup \mathcal{S},k|k^-} \mathbf{H}_{i,k}^\dagger + \mathbf{R}_{i,k})^{-1}, \\ \hat{\mathbf{x}}_{i \cup \mathcal{S},k} &= \hat{\mathbf{x}}_{i \cup \mathcal{S},k|k^-} + \mathbf{K}_{i,k}(\mathbf{z}_{i,k} - \mathbf{h}_{i,k}(\hat{\mathbf{x}}_{i \cup \mathcal{S},k|k^-})), \\ \mathbf{P}_{i \cup \mathcal{S},k} &= (\mathbf{I} - \mathbf{K}_{i,k} \mathbf{H}_{i,k}) \mathbf{P}_{i \cup \mathcal{S},k|k^-}, \\ \hat{\mathbf{x}}_{i,k} &= [\hat{\mathbf{x}}_{i \cup \mathcal{S},k}]_{1:2}, \quad \mathbf{P}_{i,k} = [\mathbf{P}_{i \cup \mathcal{S},k}]_{1:2,1:2}. \end{aligned}$$

- 4: **Belief encapsulation and broadcast:** Encapsulate the fused belief $\{\hat{\mathbf{x}}_{i,k}, \mathbf{P}_{i,k}\}$, the velocity measurement $\mathbf{v}_{i,k}$, and its timestamp $t_{i,k}$ in a CAM and broadcast.

$$\mathbf{z}_{i,k} = (\mathbf{x}_{i,k}^{\text{GNSS}\dagger}, \mathbf{z}_{\mathcal{S}_{\rightarrow i,k}})^\dagger = \mathbf{h}_{i,k}(\mathbf{x}_{i \cup \mathcal{S},k}) + \mathbf{n}_{i,k} \tag{4}$$

where $\mathbf{h}_{i,k}(\cdot)$ and $\mathbf{n}_{i,k}$ represent the mixed linear/nonlinear function of the augmented state and the measurement noise, respectively. Assume the distinct measurement noises are independent, the noise covariance matrix is given by:

$$\mathbf{R}_{i,k} = \begin{pmatrix} \sigma_{\text{GNSS}}^2 \mathbf{I}_2 & \mathbf{0} \\ \mathbf{0} & \sigma_{\text{UWB}}^2 \mathbf{I}_{|\mathcal{S}_{\rightarrow i,k}|} \end{pmatrix} \tag{5}$$

2.2. Proposed data fusion scheme

Probabilistic methods are widely considered for data fusion or state estimation [2,14]. In practice, they can be implemented in numerous ways, for instance through the Kalman Filter (KF) or its variants (e.g., EKF), or through sequential Monte Carlo methods (e.g., PF).

2.2.1. EKF-based fusion

In our data fusion context, since observations are partly nonlinear with respect to the state variables, we first consider a simple EKF-based Bayesian data fusion approach (see Algorithm 1). Vehicle i 's state belief at time t (i.e. $t_{i,k}$), which is assumed to be multivariable Gaussian, is thus represented by the mean $\hat{\mathbf{x}}_{i,k}$ and its associated covariance $\mathbf{P}_{i,k}$ (encapsulated and broadcast into CAM messages).

2.2.2. PF-based fusion

As the goodness of the linearization depends on the degree of nonlinearity of the statespace model and the degree of uncertainty of the state estimate, special care has to be taken when initializing and running the EKF in order to keep the uncertainty small [14]. PF is thus more attractive for nonlinear sequential state estimation when KF-based methods may diverge. Moreover, PF is intrinsically nonparametric with respect to the posterior density, which may be arbitrarily complex and multimodal in our case. In PF, the posterior density $p(\mathbf{x}_{i,k} | \mathbf{z}_{i,1:k})$ is approximated by a particle cloud of P random samples $\{\mathbf{x}_{i,k}^{(p)}\}_{p=1}^P$ and associated weights $\{w_{i,k}^{(p)}\}_{p=1}^P$ [14–16] i.e. $p(\mathbf{x}_{i,k} | \mathbf{z}_{i,1:k}) \approx \sum_{p=1}^P w_{i,k}^{(p)} \delta(\mathbf{x}_{i,k} - \mathbf{x}_{i,k}^{(p)})$, where $\delta(\cdot)$ is the Dirac delta function. However, it is challenging and expensive from the computation point of view to draw samples directly from $p(\mathbf{x}_{i,k} | \mathbf{z}_{i,1:k})$ due to its complex functional form [14–16]. Thus, an approximate distribution called

Algorithm 2 PF-based fusion (iteration k , “ego” vehicle i).

- 1: **CAM Collection:** Receive CAMs from the set $\mathcal{S}_{\rightarrow i,k}$ of perceived neighbors, extract the parametric beliefs, and draw samples to reconstruct the particle approximate beliefs $\{\tilde{\mathbf{x}}_{j,k < k_i}^{(p)}, 1/P\}_{p=1}^P, j \in \mathcal{S}_{\rightarrow i,k}$.
- 2: **Prediction and data synchronization:** Perform prediction of both “ego” and neighboring particle beliefs based on mobility models at the “ego” estimation instant k (i.e., $t_{i,k}$):

$$\begin{aligned} \mathbf{x}_{i,k}^{(p)} &\sim p(\mathbf{x}_{i,k} | \mathbf{x}_{i,k-1}^{(p)}), & w_{i,k|k-1}^{(p)} &= 1/P, & p &= 1, \dots, P, \\ \mathbf{x}_{j,k_i}^{(p)} &\sim p(\mathbf{x}_{j,k_i} | \tilde{\mathbf{x}}_{j,k < k_i}^{(p)}), & w_{j,k_i|k < k_i}^{(p)} &= 1/P, & p &= 1, \dots, P, & j \in \mathcal{N}_{\rightarrow i,k}. \end{aligned}$$

- 3: **Observation query and aggregation:** Check whether the TDMA MAC SF or the ranging handshakes with the subset $\mathcal{S}_{\rightarrow i,k} \subset \mathcal{N}_{\rightarrow i,k}$ of IR-UWB paired “virtual anchors” are completed to perform fusion-based CLoc:

$$\mathbf{z}_{i,k} = \begin{cases} (z_{i,k}^x, z_{i,k}^y)^\dagger, & \text{if non-fusion instant } k, \\ (z_{i,k}^x, z_{i,k}^y, \dots, \hat{z}_{j \rightarrow i,k}, \dots)^\dagger, & j \in \mathcal{S}_{\rightarrow i,k}, \text{ if fusion instant } k. \end{cases}$$

- 4: **Observation update:** Calculate the new weights according to the likelihood:

$$\begin{aligned} w_{i,k}^{(p)} &\propto \begin{cases} p(\mathbf{z}_{i,k} | \mathbf{x}_{i,k}^{(p)}), & \text{if non-fusion instant } k, \\ p(\mathbf{z}_{i,k} | \mathbf{x}_{i,k}^{(p)}, \mathbf{x}_{\mathcal{S}_{\rightarrow i,k}}^{(p)}), & \text{if fusion instant } k \end{cases} \\ &= \begin{cases} p(z_{i,k}^x | x_{i,k}^{(p)}) p(z_{i,k}^y | y_{i,k}^{(p)}), & \text{if non-fusion instant } k, \\ p(z_{i,k}^x | x_{i,k}^{(p)}) p(z_{i,k}^y | y_{i,k}^{(p)}) \prod_{j \in \mathcal{S}_{\rightarrow i,k}} p(\hat{z}_{j \rightarrow i,k} | \mathbf{x}_{j,k_i}^{(p)}, \mathbf{x}_{i,k}^{(p)}), & \text{if fusion instant } k, \end{cases} \end{aligned}$$

normalize them to sum to unity, and compute the approximate MMSE estimator and its empirical covariance as the second filter outputs:

$$\hat{\mathbf{x}}_{i,k} \approx \sum_{p=1}^P w_{i,k}^{(p)} \mathbf{x}_{i,k}^{(p)}, \quad \Sigma_{i,k} \approx \sum_{p=1}^P w_{i,k}^{(p)} (\mathbf{x}_{i,k}^{(p)} - \hat{\mathbf{x}}_{i,k})(\mathbf{x}_{i,k}^{(p)} - \hat{\mathbf{x}}_{i,k})^\dagger.$$

- 5: **Resampling:** Generate a new set $\{\mathbf{x}_{i,k}^{(p*)}\}_{p=1}^P$ by resampling with replacement P times.
- 6: **Message approximation and broadcast:** Use parametric unimodal Gaussian to approximate the particle “ego” belief and thus broadcast $(\hat{\mathbf{x}}_{i,k}, \Sigma_{i,k})$ in a CAM.

the sequential proposal density $\pi(\mathbf{x}_{i,k}, \mathbf{x}_{\mathcal{S}_{\rightarrow i,k}} | \mathbf{x}_{i,k-1}^{(p)}, \mathbf{x}_{\mathcal{S}_{\rightarrow i,k < k_i}}^{(p)}, \mathbf{z}_{i,k})$ is used instead, from which one can easily draw samples. One popular embodiment thus consists in using the mobility model as the sequential proposal density [15,16,6], i.e. $\pi(\cdot) = p(\mathbf{x}_{i,k} | \mathbf{x}_{i,k-1}^{(p)}) \prod_{j \in \mathcal{S}_{\rightarrow i,k}} p(\mathbf{x}_{j,k_i} | \mathbf{x}_{j,k}^{(p)})$.

This PF is called bootstrap PF. Our second GNSS/ITS-G5/IR-UWB data fusion scheme is thus based on such a bootstrap PF, as described in Algorithm 2.

3. Experimental setting and tested scenario

Field trials took place in Helmond, The Netherlands, in December 2017. These tests were relying on a physical proof-of-concept platform integrated in the frame of the HIGHTS project [17], consisting of three equipped vehicles (Objective’s, Tass’ and Ibeo’s in the following) forming a platoon (see Fig. 3). These vehicles made several rounds along the A270/N270 highway section. The followed route deliberately included a combination of straight and curvy portions of road.

Objective’s car was considered as the “Ego” vehicle under test, endowed with a standard GNSS (embedded in its on-board Cohda MK5 box). On the other hand, Tass’ and Ibeo’s vehicles were playing the roles of assisting vehicles (i.e. virtual anchors according to CLoc), broadcasting their own Real Time Kinematics (RTK) or/and standard GNSS information (issued by the Lidar sub-system in the latter case) over the ITS-G5 V2V channel.

The ground truth position of the “Ego” vehicle (i.e. the reference position used for performance evaluation) has been computed through a complex graph-based Simultaneous Localization and Mapping (SLAM) fusion algorithm, combining on-board RTK GNSS data, LiDAR scans and odometry data.

During these experiments, standard GNSS data were available at the “Ego” vehicle at the rate of 30 Hz. So as to limit the impact of over-oscillations (and frequent outliers/spikes) affecting these measurements, a pre-smoothing step using a sliding window of 0.2 s was applied before feeding the observation vector of the fusion filter. The ITS-G5 CAMs issued at the Cohda MK5 box (i.e. encapsulating GNSS or RTK information from the two neighboring vehicles) were received at the “Ego” vehicle at the average rate of 10 Hz. For higher fusion rates (i.e. between consecutive reception events), we could rely on mobility-based predictions to update these neighbors’ positions.

Besides, peer-to-peer ranging transactions were performed between the three cars, relying on BeSpoon’s IR-UWB devices [11]. In particular, two range measurements with respect to Tass’ and Ibeo’s vehicles were made available at Objective’s car at the rate of 10 Hz and injected into the observation vector of the fusion filter (i.e. besides standard GNSS readings). However, due to the relative instability of these ranging measurements under typical vehicular mobility (see 4.1), one simple threshold-based outliers rejection mechanism had to be implemented in the filter before performing fusion.



Fig. 3. Equipped vehicles involved in the proof-of-concept field tests.

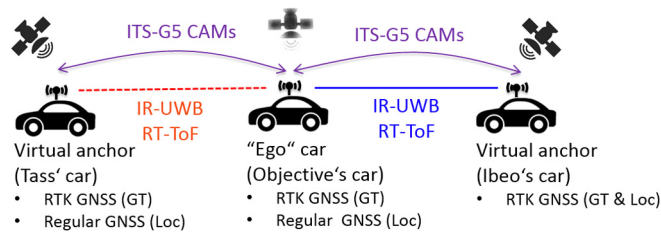


Fig. 4. Physical deployment scenario considered for both V2V ranging and V2V-aided cooperative localization testing on the field.

All in all, given the available refreshment rates and the constraints of the various input data, the best fusion rate was set to 10 Hz. For the sake of performance evaluation, representative portions of the overall test drive trajectory have been selected, lasting for approximately 30 s each, where all the desired modalities cited above were simultaneously available and sufficiently consistent.

4. Offline validation results

4.1. IR-UWB V2V ranging

Relying on the IR-UWB devices integrated platform, we first evaluate the performance of V2V ranging based on RT-ToF estimation independently. For this evaluation, we consider the same deployment scenario as that used for cooperation, illustrated on Fig. 4. In the following, note that the collected range measurements are reused as observations to feed the VA-CLoc fusion algorithm running at the "Ego" vehicle.

Fig. 5 shows the ranging estimation error as a function of time at Objective's "Ego" vehicle over one of the selected portions of trajectory, with respect to the two neighboring vehicles. It is thus shown that submetric V2V ranging accuracy can be met under practical mobility conditions, typically with a mean error equal to 0.33 m and an error standard deviation of 0.17 m with respect to Ibeo's vehicle (resp. 0.77 m and 0.33 m, with respect to Tass' vehicle).

4.2. Cooperative localization under erroneous initialization and GNSS denial

The goal is now to evaluate the effects of imperfect initialization (i.e. what we also call "cold start" herein), the relative reliability of assisting neighbors (i.e. assuming a less reliable neighbor), as well as the temporary GNSS denial at the "Ego" vehicle.

Comparing cooperative EKF and PF fusion approaches, Fig. 6 shows the bi-modal empirical Cumulative Density Function (CDF) of 2-D location errors over the selected trajectory, including both initial convergence time (as represented by approximately 20% of time with the poorest accuracy) and steady-state regime (i.e. after initial filter convergence, as represented by 80% of time with the best accuracy). Performance is assessed for "Ego" vehicle's standard GNSS alone and VA-CLoc after fusing the latter GNSS data with IR-UWB ranges and Ibeo car's RTK data and/or Tass car's standard GNSS data received

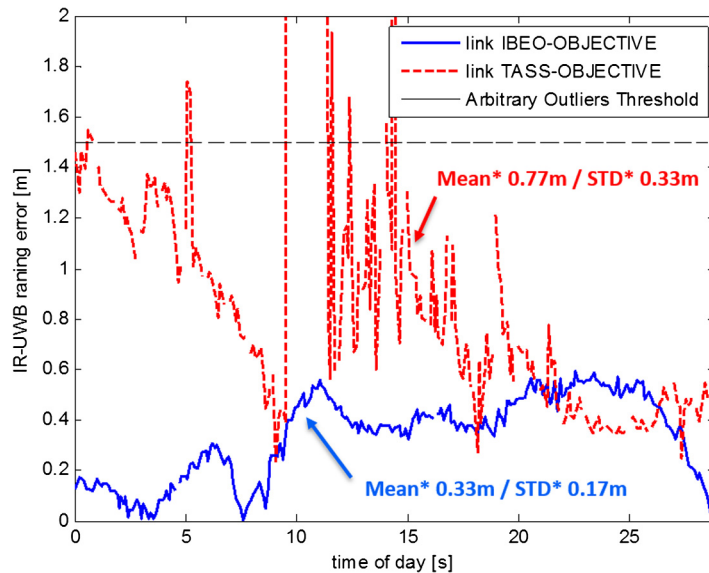


Fig. 5. RT-ToF based ranging errors as a function of time over two distinct V2V IR-UWB links (btw. “Ego” vehicle and cooperating neighbors); Empirical statistics are drawn over samples below the arbitrary outliers detection threshold (i.e. 1.5 m in the shown example).

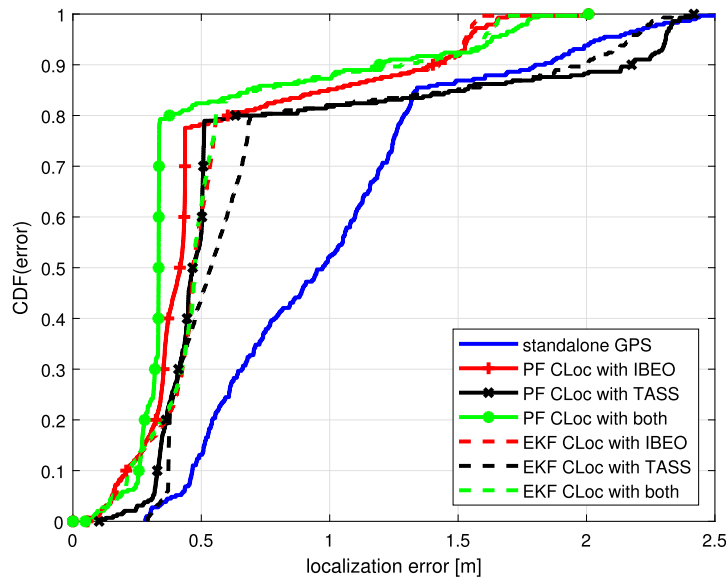


Fig. 6. Example of empirical CDF of 2-D location error at Objective's car along a selected portion of trajectory, for Cohda box's standard GNSS (blue) or VA-CLoc fusion with V2V IR-UWB range measurements and Ibeo's car's RTK only (red), Tass' Cohda box's GNSS only (black) or both neighboring cars (green) (i.e. up to 2 virtual anchors) through PF (solid) and EKF (dashed), while assuming a “cold start” at Objective's “Ego” car (i.e. initial guess only based on Cohda box's GNSS).

over ITS-G5 CAMs, while assuming initialization through standard GNSS at the “Ego” vehicle. Relying on one single GNSS-enabled neighbor (i.e. Tass), even with relatively poor ranging accuracy over the corresponding V2V link, can already boost performance in comparison with standalone GNSS once the steady-state fusion regime is reached, with a maximum error of about 0.5 m at the “Ego” after convergence, whereas considering one single RTK-enabled neighbor (Ibeo) (i.e. accounting in our case for a more reliable neighbor who would have already achieved its own fusion regime) and/or better V2V ranging performance provides an even lower error level around 0.4 m at worst (after convergence). Finally, relying on both assisting neighbors provides not only much faster convergence in the initial phase (i.e. when starting from scratch before convergence), but also additional gains in the steady-state fusion regime in terms of both error floor level and error stability, reaching typically an error around 0.3 m in the worst case (vs. 1.3 m with standard GNSS in the same conditions). Another remark is that, for all the tested cooperative configurations (i.e. CLoc with 1 or 2 assisting vehicles), PF seems to

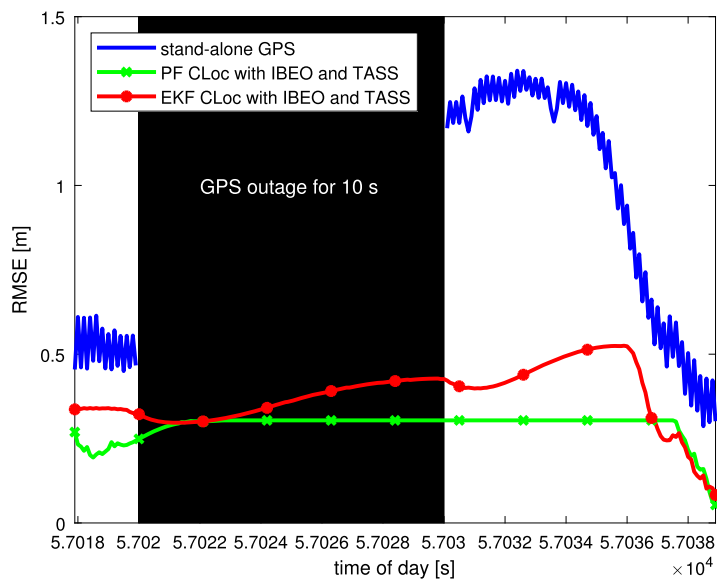


Fig. 7. Example of 2-D location error at Objective's car as a function of time along a selected portion of trajectory, for Cohda box's standard GNSS (blue) or VA-CLoc fusion with V2V IR-UWB range measurements, Ibeo's car's RTK and Tass' Cohda box's GNSS (i.e. 2 virtual anchors) through PF (green) and EKF (red) in the steady-state fusion regime, while emulating temporary GNSS denial at Objective's "Ego" car (black area).

offer better results than EKF after initial convergence, unlike in the initial convergence phase, where the two algorithms exhibit approximately the same performance level in terms of convergence speed and location error.

As a complementary result, we also show on Fig. 7 an extract of the 2-D location error as a function of time after achieving initial convergence (i.e. in the steady-state regime) for a VA-CLoc scheme involving the two assisting neighbors, while emulating a temporary GNSS loss for 10 sec at the "Ego" vehicle. One can thus note almost no performance degradation of the PF-based CLoc scheme in comparison with the initial GNSS-enabled cooperative situation, with a stable error around 0.3 m, despite still large GNSS errors beyond 1 m at the "Ego" vehicle after the end of GNSS outage, thus illustrating the resilience of the proposed solution. For comparison, the error of the EKF-based CLoc reaches 0.5 m at worst before re-converging down to the PF performance level over the same period of time.

Overall, the previous CLoc validation results tend to confirm the capability of V2V-aided cooperative localization to provide not only high accuracy, typically 30 cm in 100% of time (vs. errors beyond 1 m with standard GNSS in similar operating conditions), but also a constant quality of service, robust against occasional impairments of the standard GNSS.

5. Conclusion

In the context of vehicular ad hoc networks, we have herein introduced a Bayesian framework based on cooperative variants of the PF and EKF filters, which can perform the local fusion of on-board GNSS readings, IR-UWB ranging measurements and asynchronous ITS-G5 data with respect to neighboring vehicles. We have also provided offline proof-of-concept validations of this cooperative localization approach, based on a real system demonstrator involving three equipped vehicles. As an example, the PF-based approach has been shown to achieve quasi-constant localization accuracy around 0.3 m (at worst) in the steady-state regime after initial convergence, despite poor on-board GNSS data (with errors up to 1.3 m) or even a temporary loss of the GNSS service. These results thus confirm the relevance of V2V-aided cooperative approaches to improve both localization accuracy and small-scale service resilience for future critical C-ITS services and applications.

Beyond localization performance considerations, the current V2X transmission schemes considered to support CLoc (e.g., in ITS-G5) are mainly based on local information broadcast, so as to reach the highest number of neighboring vehicles around. As such, they are also vulnerable against both critical information leakage and/or intentional attacks, leading for instance to the denial of road safety services (ex. through jamming/spoofing, messages injection/interception, impersonation attacks...) [18,19]. So far, most of the security schemes put forward in this context rely on conventional cryptographic techniques and tools (i.e. using non-specific keys, pseudonyms or signatures), which are typically managed at the application level (e.g., foreseen for LTE-V sidelink). On the one hand, the main security features (i.e. primitives, seeds and algorithms...), which are determined in a static way, can be unsuitable into some particular vehicular use cases. On the other hand, the resulting cryptographic overhead (in terms of computational complexity and access to the core network) contributes to increase the latency of protected systems, what may be not fully compliant with local V2X interactions (possibly ad hoc) and/or even with the time-critical safety applications they are supposed to enable. Thus, lightweight and reactive cross-layer security mechanisms (e.g., adaptive authentication overlay) still need to be explored, complying with the specificity and constraints of vehicular application contexts, while reinforcing existing security schemes.

Acknowledgements

This work was partly carried out in the frame of the *HIGHTS* project, which was funded by the European Commission (636537-H2020). The authors would like to thank their colleagues from WP6 in charge of the proof-of-concept platform integration and field trials. Besides, EURECOM also acknowledges the support of its industrial members, namely, BMW Group, IABG, Monaco Telecom, Orange, SAP, ST Microelectronics, and Symantec.

References

- [1] H. Li, F. Nashashibi, Cooperative multi-vehicle localization using split covariance intersection filter, *IEEE Intell. Transp. Syst. Mag.* 5 (2) (2013) 33–44.
- [2] A. Boukerche, H.A.B.F. Oliveira, E.F. Nakamura, A.A. Loureiro, Vehicular ad hoc networks: a new challenge for localization-based systems, *Comput. Commun.* 31 (12) (2008) 2838–2849.
- [3] M. Rohani, D. Gingras, V. Vigneron, D. Gruyer, A new decentralized Bayesian approach for cooperative vehicle localization based on fusion of GPS and VANET based inter-vehicle distance measurement, *IEEE Intell. Transp. Syst. Mag.* 7 (2) (2015) 85–95.
- [4] J. Liu, B.g. Cai, J. Wang, Cooperative localization of connected vehicles: integrating GNSS with DSRC using a robust cubature Kalman filter, *IEEE Intell. Transp. Syst. Mag.* PP (99) (2016) 1–15.
- [5] S. Cruz, T. Abrudan, Z. Xiao, N. Trigoni, J. Barros, Neighbor-aided localization in vehicular networks, *IEEE Trans. Intell. Transp. Syst.* 18 (10) (2017) 2693–2702.
- [6] G. Hoang, B. Denis, J. Härrä, D. Slock, Breaking the gridlock of spatial correlations in GPS-aided IEEE 802.11p-based cooperative positioning, *IEEE Trans. Veh. Technol.* 65 (12) (2016) 9554–9569.
- [7] G.M. Hoang, B. Denis, J. Härrä, D.T.M. Slock, On communication aspects of particle-based cooperative positioning in GPS-aided VANETs, in: *Proc. CCP IV'16*, 2016, pp. 20–25.
- [8] G. Hoang, B. Denis, J. Hrri, D. Slock, Mitigating unbalanced GDoP effects in range-based vehicular cooperative localization, in: *Proc. IEEE ICC'17 - ICC Workshops*, 2017, pp. 659–664.
- [9] G. Hoang, B. Denis, J. Hrri, D. Slock, Robust and low complexity Bayesian data fusion for hybrid cooperative vehicular localization, in: *Proc. IEEE ICC'17*, 2017, pp. 1–6.
- [10] S. Severi, H. Wymeersch, J. Hrri, M. Ulmschneider, B. Denis, M. Bartels, Beyond GNSS: highly accurate localization for cooperative-intelligent transport systems, in: *Proc. IEEE WCNC18 - LCEN Workshop*, 2018, pp. 1–6.
- [11] <https://bespoon.com/>. (Accessed 15 January 2019.)
- [12] M. Petovello, K. Keefe, B. Chan, S. Spiller, C. Pedrosa, P. Xie, Demonstration of inter-vehicle UWB ranging to augment DGPS for improved relative positioning, *J. Glob. Position. Syst.* 11 (1) (2012) 11–21.
- [13] N. Drawil, O. Basir, Intervehicle-communication-assisted localization, *IEEE Trans. Intell. Transp. Syst.* 11 (2010) 678–691.
- [14] S. Thrun, W. Burgard, D. Fox, *Probabilistic Robotics (Intelligent Robotics and Autonomous Agents)*, The MIT Press, 2005.
- [15] M. Arulampalam, S. Maskell, N. Gordon, T. Clapp, A tutorial on particle filters for online nonlinear/non-Gaussian Bayesian tracking, *IEEE Trans. Signal Process.* 50 (2) (2002) 174–188.
- [16] S. Särkkä, *Bayesian Filtering and Smoothing*, Cambridge University Press, New York, NY, USA, 2013.
- [17] <http://hights.eu/>. (Accessed 15 January 2019).
- [18] E. Ben Hamida, H. Noura, W. Znaidi, Security of cooperative intelligent transport systems: standards, threats analysis and cryptographic countermeasures, in: *Special Issue Connected Vehicles, V2V Communications, and VANET*, *Electron.* 4 (3) (2015) 380–423.
- [19] H. Hasrouny, A.E. Samhat, C. Bassil, A. Laouiti, VANet security challenges and solutions: a survey, *Veh. Commun.* 7 (2017) 7–20.